

Research Article

## Experimental Investigations with Crush Box Simulations for Different Segment Cars using LS-DYNA

A.Siva Kumar<sup>A\*</sup>, G.Himabindu<sup>A</sup>, M.Sankar Raman<sup>A</sup> and K.Vijaya Kumar Reddy<sup>B</sup>

<sup>A</sup>Department of Mechanical Engineering, MLR Institute of Technology, Dundigal, Hyderabad-43,  
<sup>B</sup>Dept. of Mechanical Engineering, JNTUHCEH, Kukatpally, Hyderabad, Andhra Pradesh-85, India

Accepted 10 January 2014, Available online 01 February 2014, **Special Issue-2, (February 2014)**

### Abstract

Real time Crash testing and the Simulation of FE model are the most important sources of checking the safety of the car. The main aim of this study is for designing a crush box for different segment cars and checking its performance through numerical simulation. The companies of Insurance and the RCAR council requires the idea or technology for reducing the cost of repair and the same time improving the safety of the occupant or the passenger in the car during the Low speed impact. For reducing the cost of repair in case of Low speed crash, a special device is needed to absorb the energy caused by impact, which is called as Crush box assembly. The Crush Box is a thin-walled structure attached between the vehicle bumper structure and the side rail. The need of the Crush box is quite most important for absorbing the energy of impact. In this study, the process for crush box design development to improve the energy of absorption is proposed. The proposed process has two steps. Firstly experimental tests and numerical analysis on crush box cross sections were carried out in order to better understand their behavior and model them properly. Secondly, adding additional reinforcement and some foam types in order to satisfy different segment cars, where the difference between the segments will be the mass. The simulation of the crash itself was done by means of the Ls-Dyna code. The optimized design of crush box will be designed which should absorb more energy during RCAR Crash performance. According to the RCAR rule, the simulation at low-speed impact of 16km/h was carried out to evaluate the crashworthiness of the car.

**Keywords:** Polymer Matrix Composites, Injection Moulding, Flexural Strength, Hardness.

### 1. Introduction

Crashworthiness simulations have significantly contributed to the enhancement of safety in modern vehicles. Additionally the desire of manufacturers to shorten design cycles for vehicle was only possible because of Computer Aided Engineering (CAE) analysis. Several crash cases have to be examined. For example, Frontal impact with different off-set values, Side impact of barriers with varying velocities, low speed collisions or the flashover of a car. Now-a-days, very detailed models with a huge amount of elements allow reliable predictions on the endangerment of occupants

#### 1.1 Frontal Crash

Increased traffic intensity, growing concern of the general public, and more stringent legislation have made vehicle safety one of the major research areas in automotive engineering. An area of particular concern is the early crashworthiness design of cars. Cars have to pass the compulsory crash test as issued by the authorities. However, this test does not guarantee that cars are safe in crash situations that deviate from the prescribed one.

Hence, the entire collision spectrum within which the car must be safe must be investigated as shown in the Fig.1

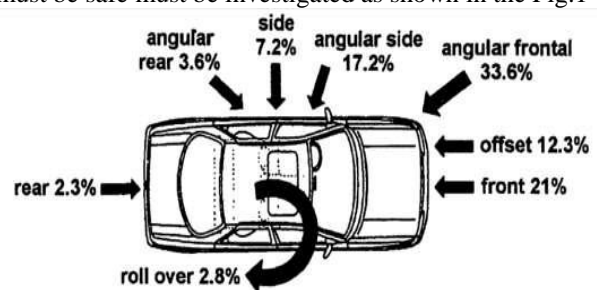


**Fig.1** Various Types of Crash

#### 1.2 Structure Introduction

The recent economical global crisis and the continuing unstable prices of oil and raw materials have tended the manufacturer to reduce the weight of automobiles and increase the efficiencies of engines, transmission and active and passive safety systems. The body in white of automobile using the combination of various kinds of materials including high strength steels, aluminum sheet/extrusions and casting, magnesium castings and carbon fiber reinforced plastics as shown in the Fig.2

\*Corresponding author: **A.Siva Kumar**



**Fig.2** Body in white structure (BIW)

A crash element should transform the kinetic energy into the deformation energy in a controllable manner, retain sufficient survival space for the protected components and keep the forces and accelerations on the crash element. In the automobiles, percentage of the occurrence of the frontal crashes is shown to be about 70% including direct and offset frontal crashes.

A crash box is an element which is used in the frontal crash zones, generally inserted between chassis and bumper as shown in Fig.3&4. Crash boxes absorb the total crash energy at velocities approximately up to 30 km/h and protect the overall integrity of chassis and transmit less amount of energy to the rest of the front safety zones at velocities higher than 30km/h.



**Fig.3** Bumper, crash box, engine and chassis positions



**Fig.4** Different types of crash boxes in various geometries

## 2. Methodology and Improvements

Two methodologies have been recently applied to improve the energy & absorption performances of crash boxes. These are the use of multiple-cell structure and filling the crash boxes with a with light-weight metallic foam. Aluminum foam filling particularly has received much interest from both academia and industry since they have

relatively very low density as compared with the foams of other metals.

## 3. Results

### 3.1 Design of Energy absorbing Crash Boxes

For the design of a car structure that has to sustain a frontal collision, multiple aspects must be considered, i.e. collision velocity, crash direction, overlap percentage, and obstacle type. The energy dissipation in a frontal crash normally occurs by deformation of the longitudinal members. These must absorb a large part of the kinetic energy.

The design spectrum for a longitudinal member is further analyzed and a set of design requirements is formulated. With the aid of Finite Element Method (FEM) models of several longitudinal cross-sections, numerical simulations have been executed to evaluate the influence of the design parameters on the crash behavior.

### 3.2. Parameters as design requirements for Simulations

To enable the geometric design of the longitudinal members, it must first be clear what kind of loads can occur in real frontal collisions. These loads are determined by the parameters describing the frontal crash and their predominant values. Besides the collision speed, the obstacle type, the impact location and direction, also the vehicle mass has a large influence on the crash behavior. An average car with two occupants and luggage has a mass of approximately 1100 kg.

The goal for these simulation studies is to find a single geometric profile. To limit the amount of simulations, the following simplifications were chosen in relation to the above mentioned parameters:

1. Two collision speeds, viz. 28 and 56 km/h.
2. Obstacle type: only rigid walls, although a deformable barrier is more realistic, it has a disadvantage in comparing energy absorption's of different geometry's.
3. Two extreme overlap percentages, to be sure a crash load will lead to acceptable energy absorption in extreme crash configurations:
  - a. Full overlap (two longitudinal members and the engine are loaded)
  - b. 40 per cent overlap (only one longitudinal member is loaded)
4. Three impact directions: 0, 15 and 30 degrees.
5. Two vehicle masses: 550 and 1100 kg. The effective mass for a single longitudinal member depends on the specific impact location.

### 3.3. Results of Simulations

The material selected for the five mentioned profiles was commonly used steel (for specifications see Table). Over the length of the longitudinal member, the profile thickness was kept constant at 2.0 mm. This value is realistic and generally gives a stable folding pattern. The dimensions of the profiles were chosen to have the same parameter resulting in a constant mass per unit of length as

shown in Table 1. The undeformed length of each profile is 350 mm.

**Table 1:** Various Profile Shapes

Profile	Shape
A	square
B	rectangle
C	circle
D	hexagon
E	octagon

The results of the simulations, which concern a collision with a 56 km/h impact speed, a mass of 1100 kg, and a normal angle of incidence. Both extremities of the column have an undeformable plate (rigid body), this is more realistic (normally they have a connection with stiffer vehicle components) and better for mutual comparison and to exclude different end effects. The energy absorption is plotted as function of the deformation length (rather than a function of time) because this facilitates the comparison of different structural design concepts. With the deformation length is meant the shortening of the profile. The simulation was terminated at the moment that the load shows a large increase as a result of reaching the maximum available deformation length as shown in the Fig.5.

Based upon these five simulations, it can be concluded that a square and a rectangular profile have significantly lower energy absorption than the other three profiles. The octagonal profile absorbs slightly more energy during the deformation than the circular and the hexagonal profiles, which absorb nearly the same amount of energy. The circular profile yields the longest possible deformation length and, hence, is capable of absorbing slightly more energy in its final deformation. Note that there were no geometrical imperfections used and the folds have to fit between the undeformable extremities.

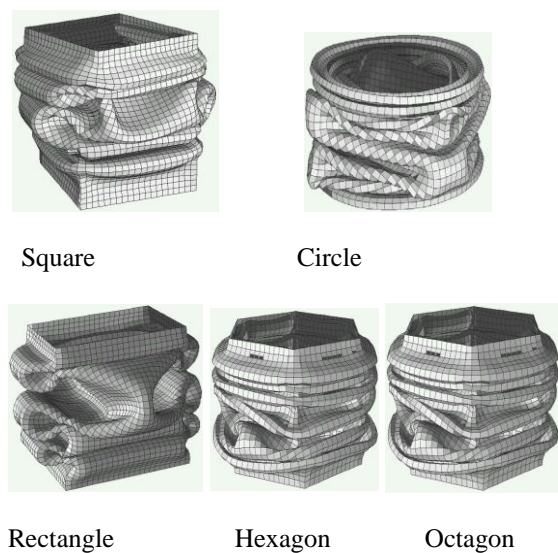


**Fig.5** Profiles with a Different Cross-Section

3.4. Design of triggering for stable force

A stable force level of the crushing column over the whole length can be reached by triggering of the beam. By applying specific weaknesses on the proper position at the front end of the beam, a stable regular folding process will start at that position without a much higher peak force level to introduce the first fold. These crash initiators prevent overly high loads, which could cause a bending collapse of the still long undeformed length, or other not programmed deformations of the structure. The folding process starts controlled at the front end and proceeds regularly towards the rear end, giving more stability. In this case, the whole length of the column could be used for folding lobes of the same size, finally leading to the highest energy absorption. In the case of bending, only a few folds could be formed. See below Figures for the difference in deformation between an equal square crash column of 1160 mm length and one with and the other without triggering for an axial load. The perimeter is 300 mm and the wall thickness is 2.0 mm. For clearness the right picture is zoomed in. Note that this is a special example with a relatively long column, yielding lateral buckling of the not triggered column. In case of a shorter column where no lateral buckling occurs, the final difference in energy absorption is smaller.

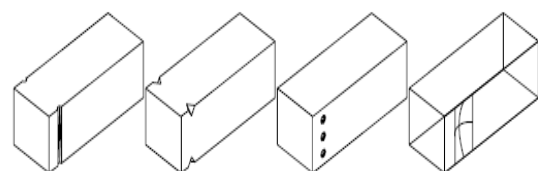


Column without triggering    Column with front triggering

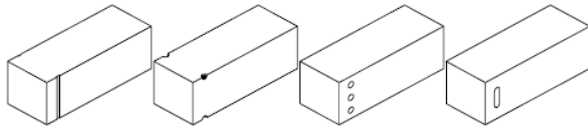
The energy absorption of both longitudinal is compared. Because the column without crash initiators is stiffer, it absorbs more energy during the first deformation part but afterwards the additional energy absorption is strongly reduced by bending, resulting in a lower overall energy absorption. In much lower force level of the triggered beam can be seen at the start of the crash.

3.4.1. Determination of trigger geometry efficiency

Two types of crash initiators are researched, weaknesses formed by pressing a stamp into the wall or corner, or weaknesses formed by punching (taking material away). All simulations are done with a square column of 75x75x2 mm with a rigid front end and with a crash speed of 56 km/h, resulting in an initiator distance of  $\frac{1}{2} \times 44 = 22$  mm. In the upper row of below figures, four stamp forms are shown and in the lower row four punch forms.



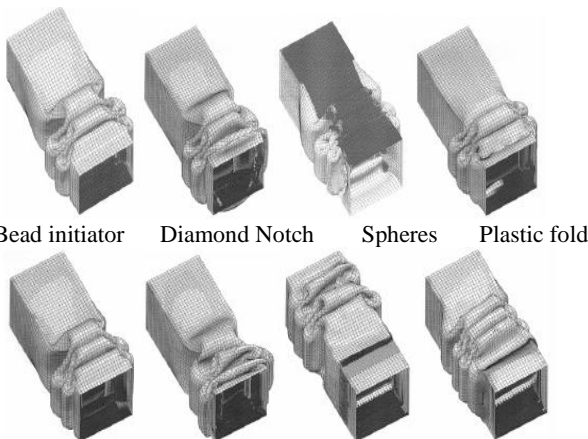
Bead initiator    Diamond Notch    Spheres    Plastic fold



Smaller Thickness Circular Notch Circular Holes Oval Hole

**Table 2:** Various loads

Initiator form	First peak load [kN]	Energy absorption [J]
no initiator	216	15323
bead	155	11099
diamond notch	179	12473
spheres	183	11534
plastic fold	175	11680
smaller thickness	191	13623
circular notch	170	12300
circular holes	196	12211
oval hole	191	12030



Bead initiator Diamond Notch Spheres Plastic fold

Smaller Thickness Circular Notch Circular Holes Oval Hole

From these pictures, it is clear that especially the notches on the corner and the both forms with holes are not stable. The relative stiff corners of a square column must not be weakened, because this weakening could cause a small rotation or translation of the whole cross-section. If a deviating fold is formed, it disturbs all next folds with a much higher risk of a bending collapse due to the decreasing moment of inertia.

Based on the lowest first peak level, the most regular force curve with expected wavelength and the very stable folding pattern as visible, the bead initiator must be preferred as most suitable trigger form.

**3.5. Simulation of Empty and Foam Filled Crash Box**

Al alloy was modeled with 4 node Belytschko–Tsay shell elements with one point integration in the plane and five in the thickness direction. 8-node solid elements were used to model Al foam. The shell and solid element lengths were taken 3 and 6 mm, respectively. LS-DYNA is based on explicit time integration 88 and since the quasi-static deformation occurs under relatively low deformation rates, the quasi-static modeling in LS-DYNA requires relatively long durations. To simulate the quasi-static deformations

at reasonably shorter times in LS-DYNA, the mass scaling is usually applied. In the simulation of the quasi-static crushing of empty and filled boxes, the material mass density was scaled down by a factor of 1000 and the deformation speed was increased to 2 m s<sup>-1</sup>. Dynamic crush simulations results of G1 geometry boxes (implemented with the montage plates) were used as inputs to the crash boxes optimization. In dynamic simulations, a planar moving force contact algorithm was used to simulate the impact of 550 kg mass with an initial deformation velocity of 10 ms<sup>-1</sup>.

In the quasi-static compression simulations, the compression top and bottom plates were modeled as rigid walls. The planar forces and the geometric flat motion of rigid wall algorithms were applied to top and bottom compression plates, respectively. In the modeling of the deformation of empty and partially filled aluminum crash boxes without additional plates, the planar flat rigid wall representing the bottom deformation plate was fixed, no translation and rotation, and the geometric flat motion rigid-wall representing the upper plate moved only in z direction, the motion in all other directions was restricted. In the simulation of empty and partially filled crash boxes with additional parts; however, no rigid wall algorithms were used. The top and bottom weld plates were created as separate parts and the bottom and top weld plates were constrained. Since the width of the welding zone was measured 9 mm, the rotational motions of all nodes in a distance 6 mm from the top and bottom of tube were not allowed in all direction . The translation motion of weld zone nodes was only allowed in Z direction. Similar constraints were also previously applied in the simulation of the crushing of 5018 Al tubes .

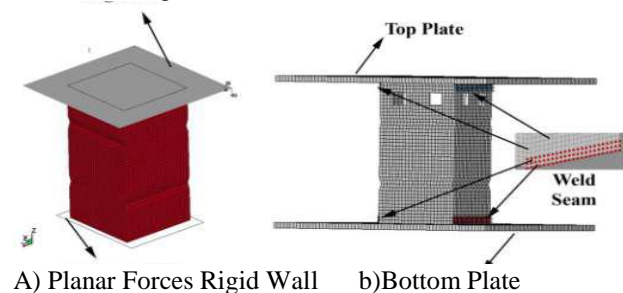


**Fig.6** Geometric Flat Motion Digid Wall

The model of a) crash box without additional plates and b) Crash box with additional plates.

The self contact of crush zone surfaces (contact between folds) was modeled with automatic single surface contact algorithm .Automatic surface to surface contact algorithm was used to simulate the contact between foam filler and box wall and box edge and weld plates of crush boxes with montage plates (The contact between crash zone and additional plates was modeled with automatic nodes to surface contact algorithm.

**3.6. Empty & Partially Foam Filled Simulation without Additional Parts**

The pictures of the deformation sequences of empty and

partially Alulight foam filled 1050 H14 Al crash boxes without additional parts. Quasi-inextensional deformation mode is observed in all numerically crushed empty boxes . As similar the numerical number of fold formation increases in partially foam filled boxes. Load and mean load-displacement curves of empty and F1 and F2 partially Alulight foam filled 1050 H14 Al crash boxes without additional parts . The numerical load and mean load-displacement curves essentially show good agreements in empty and filled 2 and 3 mm thick crash boxes, while the numerical mean load values of the 2.5 mm thick crash boxes are slightly higher than those of experiments. The weld seam opening is observed during the compression loading of few empty tubes. However, no significant effect of weld seam opening is detected on the load-displacement curves. The weld seam opening occurs at a later stage of the fold formation and therefore its influence, if any, on the load values is relatively small at increasingly large displacements as seen the following figures from Fig.7 to 15.

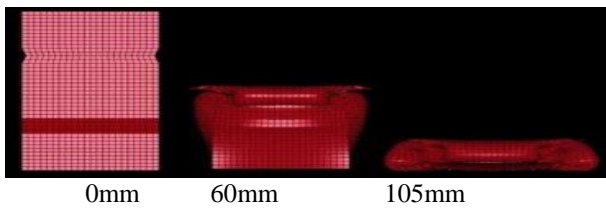


**Fig.7** Sequential deformation photos of empty crash box without additional parts,  $t=3$  mm (G1T3E).

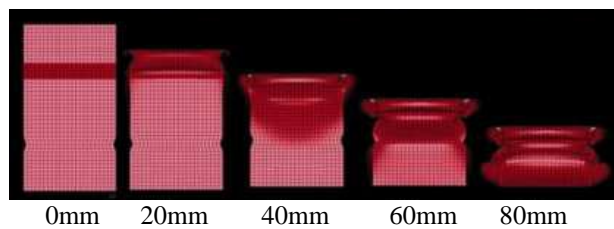


**Fig.8** Sequential deformation photos of filled crash box without additional parts,  $t=3$  mm (G1T3F1).

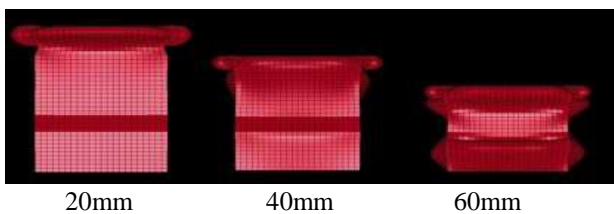


**Fig.9** Sequential deformation photos of filled crash box without additional parts,  $t=3$  mm (G1T3F2).

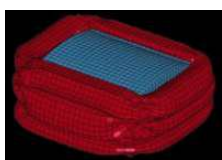


**Fig.10** Deformation photo of filled crash box without additional parts,  $t=2$  mm, (G1T2F2).

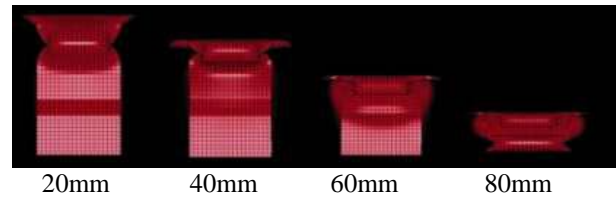


**Fig.11** Sequential deformation photos of empty crash box without additional parts,  $t=3$  mm (G2T3E).

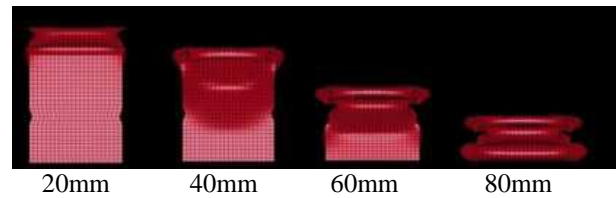


**Fig.12** Sequential deformation photos of filled crash box without additional parts,  $t=3$  mm (G2T3F1).

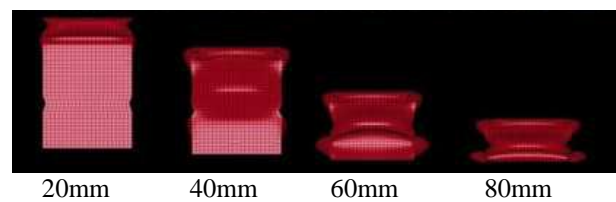


**Fig.13** Sequential deformation photos of filled crash box without additional parts,  $t=3$  mm (G2T3F2).



**Fig.14** Deformation photos of empty and filled crash box without additional parts,  $t=2.5$  mm (G2T2.5E)

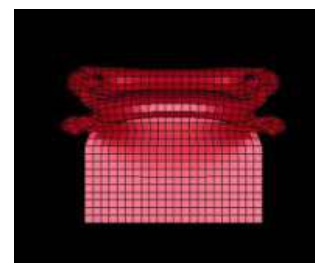
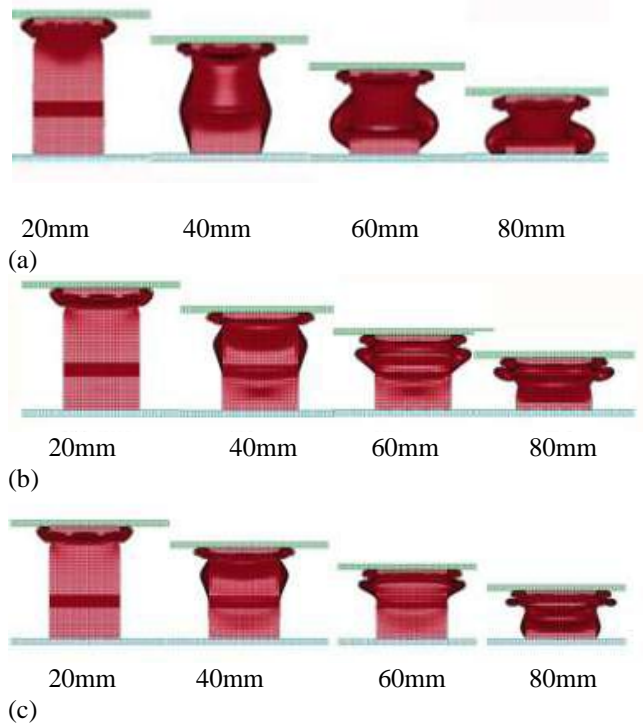


**Fig.15** deformation photo of filled crash box without additional parts,  $t=2$  mm, (G2T2F1).

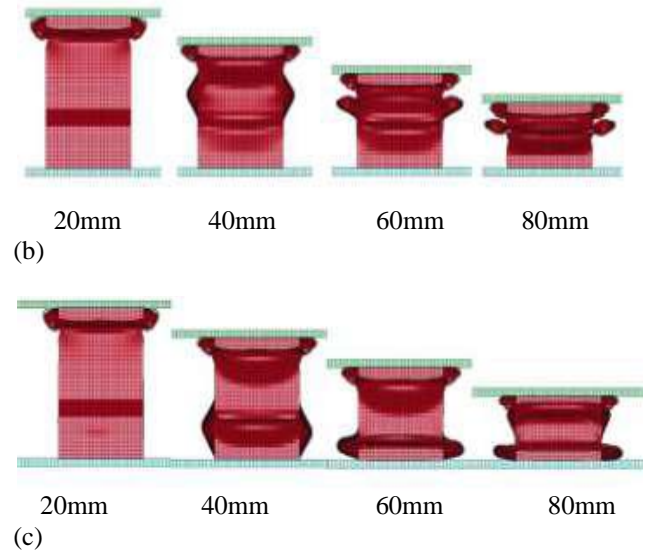
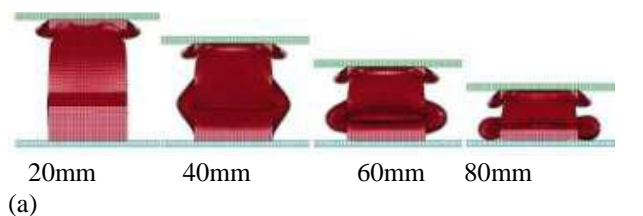
*3.7. Empty & Partially Foam Filled Crash Box Simulation with Additional Parts*

The numerical and experimental pictures of the deformation sequences of empty and partially F1 and F2 Alulight foam filled G1 geometry 3 mm, 2.5 mm and 2 mm thick 1050 H14 Al crash boxes with montage parts are

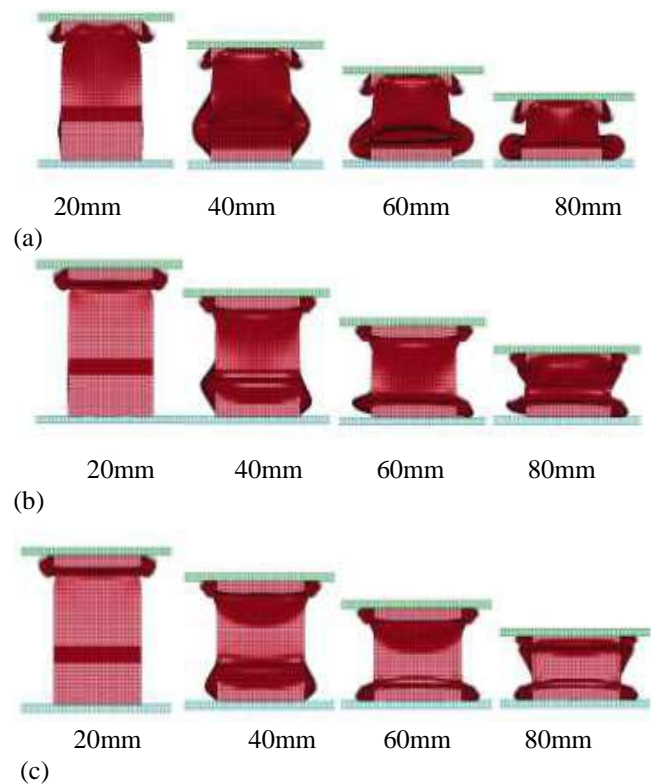
shown in Fig.16,17,18 respectively. As shown in Fig.16 foam filled G1 geometry boxes with 3 mm thickness deform in progressive folding mode both experimentally and numerically. G1 box geometries in 2.5 and 2 mm thickness, the deformation is non-progressive (Fig.17& 18). The numerical and experimental pictures of the deformation sequences of empty and partially F1 and F2 Alulight foam filled G2 geometry 3 mm, 2.5 mm and 2 mm thick 1050 H14 Al crash boxes with montage parts are shown in Fig.19, 20 & 21, respectively. Similar to 2.5mm and 2 mm thick foam filled G1 boxes, all G2 geometry filled boxes deform in non-progressive mode. It is also noted that, the folding starts in the empty top and bottom sections of the foam filled crash boxes, followed by the folding of the foam filled section. Similar to crash boxes without montage part, foam filling in boxes with montage plates increases the total number of fold formation. The experimental and numerical load and mean load-displacement curves of empty and partially F1 and F2 Alulight foam filled G1 and G2 geometry crash boxes with montage parts are shown in Figures respectively. However, the initial peak load values are still the maximum loads in empty tubes. In the filled tubes however, the second fold induces numerically a higher peak load value than initial peak load mainly due to interaction between the foam filler and crash box.



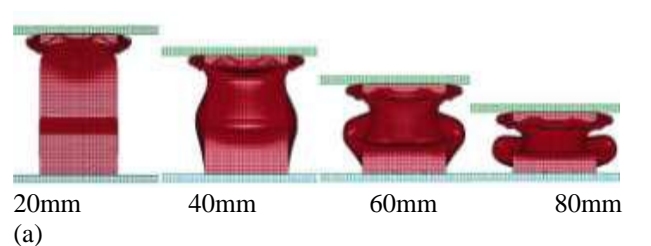
**Fig.16** Sequential deformation pictures of crash box with additional parts a) empty, b) F1 foam filled and c) F2 foam filled (Geometry G1, t =3 mm).



**Fig.17** Sequential deformation pictures of crash box with additional parts a) empty, b) F1 foam filled and c) F2 foam filled (Geometry G1, t= 2.5 mm).



**Fig.18** Deformation pictures of crash box with additional parts a) empty, b) F1 foam filled and c) F2 foam filled (Geometry G1, t= 2 mm).



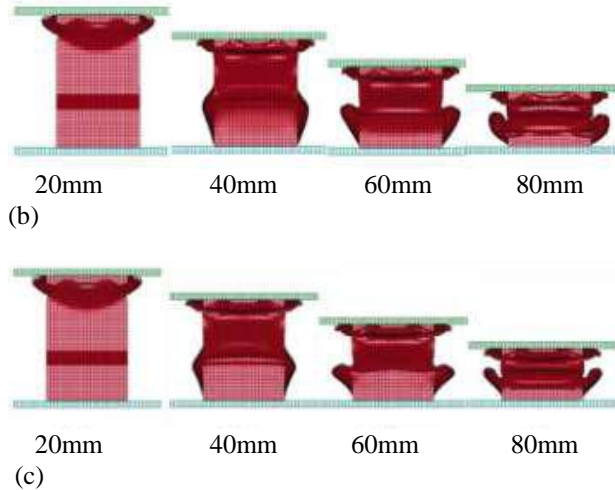


**Fig.19** Deformation pictures of crush box with additional parts a) empty, b) F1 foam filled and c) F2 foam filled (Geometry G2, t= 3 mm).

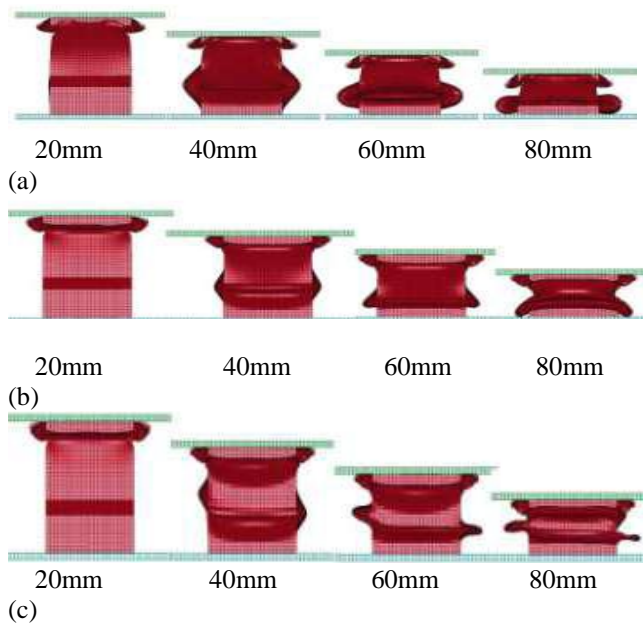


**Fig.20** Deformation pictures of crush box with additional parts a) Empty, b) F1 foam filled and c) F2 foam filled (Geometry G2, t= 2.5 mm.)

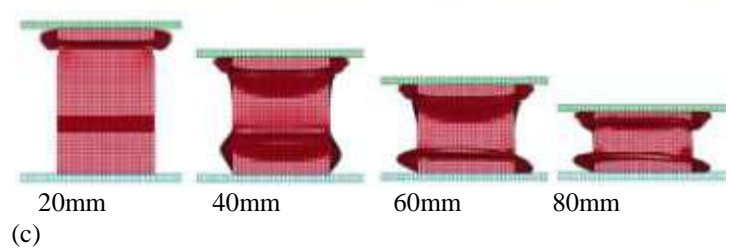
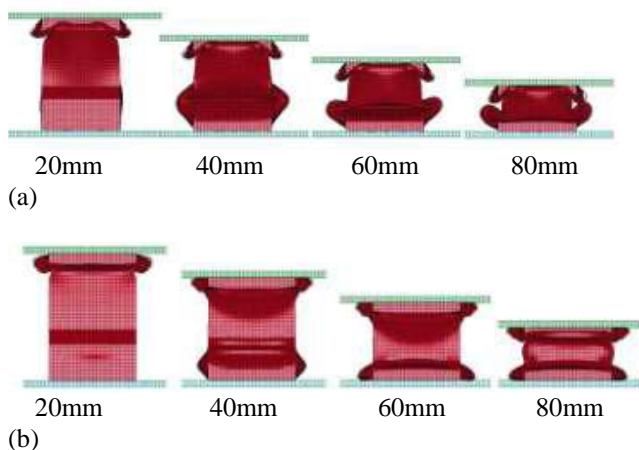


**Fig.21** Deformation pictures of crush box with additional parts a) empty, b) F1 foam filled and c) F2 foam filled (Geometry G2, t= 2 mm)\

**Conclusions**

- Crush box components absorbing energy are studied through basic types of different cross sections.
- Square and Rectangular profile have significant Lower energy absorption than the other profiles
- The method of triggering the energy absorption was studied using Rectangular type profile, so that one type of profile can be commonly used in cars.
- The bead initiator must be preferred as most suitable trigger form with good efficiency.
- Results are tabulated and compared with various improvements.
- The final tabulated values are given to other departments like NVH, DURABILITY for further clarification on their regulations.
- More study on different material foam and improvements in additional can achieve more improvement on deformation and energy absorption
- Crush box with foam material and additional parts can be used with cars with high mass and without foam & additional parts can be used in small cars
- Suitable alternative is suggested based on results obtained for various alternatives undertaken.

**References**

Marcus Redhe and Larsgunnar Nilsson , Engineering Research Nordic AB Shape Optimization of Vehicle Crush box using LS-OPT  
 Liu Yanjie1, Ding Lin Computer simulations and experimental study on crash box of Automobile in low speed collision  
 Hao Yan, The low-speed car collision, Automotive and accessories (2003)  
 Research Council for Automobile Repairs, Vehicle Design Features for Optimum Low Speed Impact Performance, (1995)  
 L. Ramon-Villalonga, Th. Enderich Advanced Simulation techniques for Low Speed Vehicle Impact  
 LS-DYNA, Keyword User's Manual, Version 971 Livermore, Livermore Software Technology Corporation, and also www.dynasupport.com  
 LS-OPT User's Manual version 2.2, Livermore, Livermore Software Technology Corporation, and also www.dynasupport.com  
 Hypermesh version 8.0, Altair Inc, Troy 2004